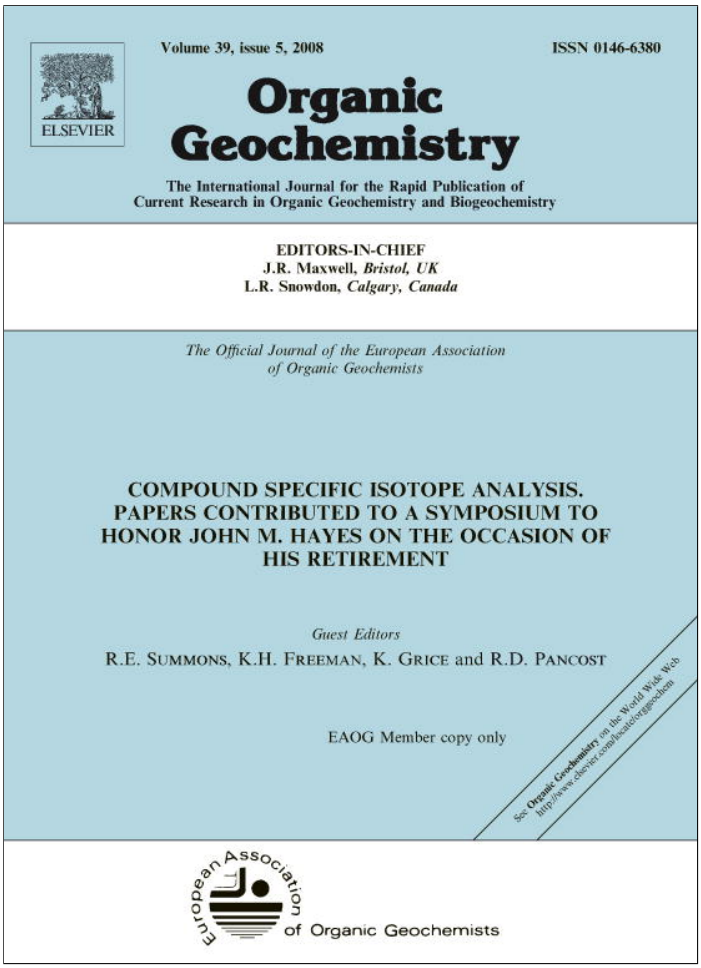

Available online at www.sciencedirect.com
ScienceDirect
Organic Geochemistry 39 (2008) 532–549
Organic Geochemistry
www.elsevier.com/locate/orggeochem

Diazotrophic cyanobacteria as the major photoautotrophs during mid-Cretaceous oceanic anoxic events: Nitrogen and carbon isotopic evidence from sedimentary porphyrin

Yuichiro Kashiyama [a,b,*], Nanako O. Ogawa [b], Junichiro Kuroda [b], Motoo Shiro [c], Shinya Nomoto [d], Ryuji Tada [a], Hiroshi Kitazato [b], Naohiko Ohkouchi [b,*]

[a] *Department of Earth and Planetary Science, The University of Tokyo, Tokyo 113-0033, Japan*
[b] *Institute for Research on Earth Evolution, Japan Agency for Marine-Earth Science and Technology, 2-15 Natsushima-cho, Yokosuka 237-0061, Japan*
[c] *X-ray Research Laboratory, Rigaku Co., Akishima 196-8666, Japan*
[d] *Department of Chemistry, University of Tsukuba, Tsukuba 305-8571, Japan*

Received 1 March 2007; received in revised form 5 November 2007; accepted 27 November 2007
Available online 24 January 2008

Abstract

We determined both the nitrogen and carbon isotopic compositions of nickel-chelated deoxophylloerythroetioporphyrin (Ni DPEP), a major sedimentary porphyrin extracted from the Livello Selli and Livello Bonarelli black shales deposited in the western Tethys Sea during mid-Cretaceous oceanic anoxic events (OAEs). Based on empirical isotopic relationships between the tetrapyrrole nuclei of chlorophylls and photoautotroph cells, we estimate that the mean nitrogen isotopic composition of the entire photoautotrophic communities during these periods ranged from −2‰ to +1‰. This result strongly suggests that N_2-fixation was an important primary process in photoautotrophic production during these OAEs. The estimated carbon isotopic composition of the photoautotrophs was elevated (between −20‰ and −22‰) relative to typical Cretaceous examples, indicating as much as a 5‰ reduction in the magnitude of carbon isotopic fractionation associated with photosynthesis during OAEs in the western Tethys Sea. This anomaly can be well explained if cyanobacteria were the dominant producers because they commonly conduct β-carboxylation and/or active transport of carbon substrates, resulting in reduced carbon isotopic fractionation. We therefore conclude that diazotrophic cyanobacteria were the dominant components of primary production during OAE-1a and OAE-2 in the western Tethys Sea.

1. Introduction

The global deposition of dark-colored carbon-rich organic sediments (i.e., "black shales") occurred repeatedly during mid-Cretaceous oceanic anoxic events (OAEs; Schlanger and Jenkyns, 1976).

* Corresponding authors. Address: Institute for Research on Earth Evolution, Japan Agency for Marine-Earth Science and Technology, 2-15 Natsushima-cho, Yokosuka 237-0061, Japan. Tel.: +81 468 67 9805; fax: +81 468 67 9775.
E-mail addresses: chiro@jamstec.go.jp (Y. Kashiyama), nohkouchi@jamstec.go.jp (N. Ohkouchi).

0146-6380/$ - see front matter © 2007 Elsevier Ltd. All rights reserved.
doi:10.1016/j.orggeochem.2007.11.010

The paleoenvironment and ocean dynamics of these unusual OAEs have been investigated in an effort to understand their cause and consequences. Previous arguments have commonly called for one of the following two mutually exclusive mechanisms in explaining the formation of apparently anaerobic deep water and the accompanying exceptional preservation of organic matter: amplified biological production by upwelling, and oceanic stagnation (Pederson and Calvert, 1991; Arthur and Sageman, 1994).

Previous studies have identified an unusual aspect of the surface water ecology during OAEs; namely, the significant contribution of cyanobacteria to primary production. Ohkouchi et al. (1997) determined the nitrogen isotopic composition of bulk samples from the Livello Bonarelli black shale deposited during OAE-2 (latest Cenomanian). The authors concluded that the low observed $\delta^{15}N$ values (−2‰ to +0.6‰), in combination with a great abundance of hopanoids, reflected N_2-fixation by cyanobacteria. Recently, Kuypers et al. (2004) suggested that cyanobacteria were the major primary producers during OAE-1a (early Aptian) in the Tethys Sea and Pacific Ocean (DSDP Site 463) and during OAE-2 in the proto-North Atlantic, as deduced from previous findings of the abundance of 2-methylhopanoids, a cyanobacterial lipid biomarker (Summons et al., 1999). Dumitrescu and Brassell (2006) also suggested a major contribution of cyanobacterial organic matter to OAE-1a black shale from the Pacific Ocean (Shatsky Rise, ODP Leg 198), again based on an abundance of 2-methylhopanoids. More recently, Ohkouchi et al. (2006) made a robust argument for the significant contribution of diazotrophic cyanobacteria during OAE-2, as deduced from the $\delta^{15}N$ values of sedimentary porphyrins (chlorophyll-derived compounds).

The present study reports on both nitrogen and carbon isotopic data for sedimentary porphyrins, providing further constraints on the photic zone environment during mid-Cretaceous OAEs. Although sedimentary porphyrins are potentially derived from both chloropigments and hemes (Treibs, 1936; Baker and Louda, 1986; Boreham et al., 1989; Ocampo et al., 1989; Callot and Ocampo, 2000), those observed in pelagic sediments are likely to have been derived mainly from chloropigments produced as antenna pigments by marine photoautotrophs (Baker and Louda, 1986; Keely et al., 1990; Eckardt et al., 1991). Such porphyrins retain the original isotopic compositions of the chloropigments, thereby strongly reflecting the isotopic compositions of the source photoautotrophs (Hayes et al., 1987; Boreham et al., 1989, 1990; Ocampo et al., 1989; Popp et al., 1989; Chicarelli et al., 1993; Keely et al., 1994; Ohkouchi et al., 2006). Specifically, the nitrogen isotopic composition of photoautotrophs reflects the nitrogen substrate and its process of assimilation during growth, thereby making such data useful in reconstructing the nitrogen cycle of paleo-oceans (e.g., Sachs and Repeta, 1999a; Sachs et al., 1999b; Ohkouchi et al., 2006; York et al., 2007). For example, Chicarelli et al. (1993) reported a low nitrogen isotopic composition for various porphyrins from the Triassic Serpiano oil shale, and inferred that N_2-fixing cyanobacteria were the predominant primary producer within the paleoenvironment. The carbon isotopic composition of photoautotrophs also reflects the nature of carboxylation processes and related physiological, taxonomic, and environmental factors (e.g., Popp et al., 1989; Hayes, 1993; Bidigare et al., 1997; Pancost et al., 1997; Pagani et al., 1999a,1999b, 2002). Isotopic analyses of sedimentary porphyrins therefore provide a crucial tool in elucidating the physiology of photoautotrophs, their role in biogeochemical cycles, and the paleoenvironment of the surface ocean.

In the present study, we analyzed two representative OAE black shales deposited in the western Tethys Sea: the Livello Selli and Livello Bonarelli black shales, corresponding to OAE-1a (early Aptian) and OAE-2 (latest Cenomanian), respectively. These two OAEs are of great significance because of their global distribution (see Kuroda and Ohkouchi, 2006 and references therein). In the present work, we report on the carbon and nitrogen isotopic compositions of nickel-complexed deoxophylloerythroetioporphyrin (Ni DPEP), one of the major porphyrins found in these shales. The chemical structure of DPEP indicates that it can potentially be derived from most varieties of chloropigments; in practice, however, it represents chlorophyll *a*, which is the sole quantitatively important chloropigment produced by virtually all of the oxygenic photoautotrophs as their *major* antenna pigment. Therefore, we regard the nitrogen and carbon isotopic compositions of DPEP to reflect the mean values of the entire photoautotrophic community in the paleo-ocean. Based on isotopic data for Ni DPEP, we discuss

the physiology of the photoautotrophs and associated biogeochemical cycles in the western Tethys Sea during the mid-Cretaceous OAEs.

2. Geological setting and samples

The Livello Selli and Livello Bonarelli black shales, which consist dominantly of organic rich pelagic shale, occur within a thick mid-Cretaceous chalk bed. The Livello Selli shale and associated chalk make up the Marne a Fucoidi Formation, while the Livello Bonarelli shale and associated chalk make up the Scaglia Bianca Formation. These formations, together with underlying and overlying strata, constitute the Early Jurassic–Paleogene pelagic carbonate sequence (1300–2000 m thick) of the Marchen Apennines, central Italy (Cresta, 1989; Coccioni and Luciani, 2004; Kuroda et al., 2005). At the time of deposition, the basin was located in the center of the western Tethys Sea (Arthur and Premoli Silva, 1982).

The Livello Selli black shale is recognized as one of the representative layers of OAE-1a, whereas the Livello Bonarelli black shale corresponds to OAE-2 (Schlanger and Jenkyns, 1976; Jenkyns, 1980; Arthur et al., 1990; Kuroda et al., 2007). Both OAE-1a and OAE-2 are known for the worldwide deposition of organic-rich anaerobic sediments, not only throughout the entire western Tethys but also in the North and South Atlantic, Western Interior Seaway, and Central Pacific (Pratt, 1984; Schlanger et al., 1987; Philip et al., 1993, 2000; Meyers et al., 2001; Kuroda and Ohkouchi, 2006). OAE-2 also marks the largest biotic crisis during the

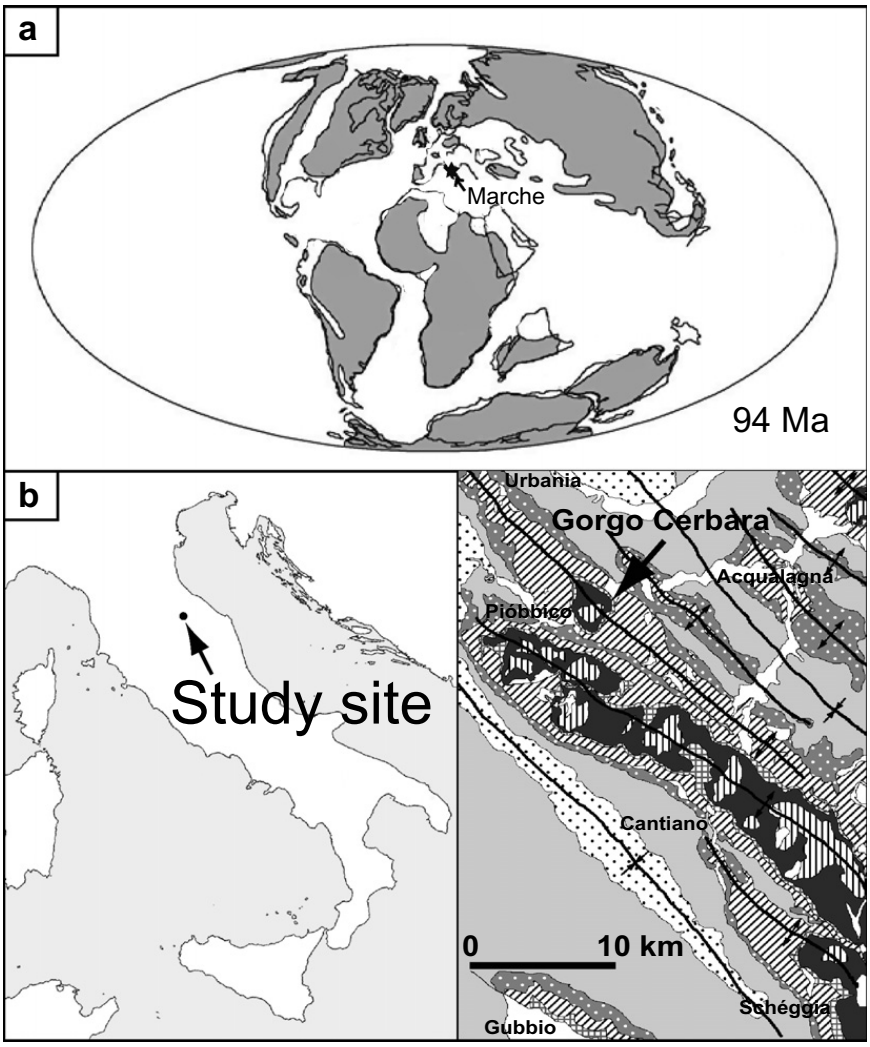

Fig. 1. (a) Paleogeography of the mid-Cretaceous (94 Ma; after Scotese and Golonka, 1992), showing the study area. (b) Locality maps of the Gorgo Cerbara section.

Mesozoic Era (Hallam and Wignall, 1999). Positive excursions of the carbon isotopic composition of sedimentary carbonates and organic matter are known across these OAE intervals, interpreted to reflect the enhanced sequestration of ^{13}C depleted organic carbon into the sediment (Schlanger and Jenkyns, 1976; Jenkyns, 1980; Arthur et al., 1987, 1988).

The samples analyzed in the present study were collected from the Gorgo Cerbara section, Marche, central Italy (Fig. 1). In the studied section, the Livello Selli black shale is 200 cm thick, consisting of alternating centimeter scale layers of dark organic rich shale and greenish gray shale (Fig. 2a). The sample obtained from this unit is organic rich black shale obtained from the upper part of the section (Fig. 2a). The Livello Bonarelli black shale is 100–120 cm thick in this section, and consists of alternating centimeter scale layers of dark organic rich shale and light organic poor shale/siliceous shale separated along sharp boundaries (Fig. 2b). The lithology and stratigraphy of this section is described in detail by Kuroda et al. (2005). Four organic rich layers of siliceous black shale (Levels A–D in Fig. 2b) within the Livello Bonarelli black shale were sampled and analyzed in this study.

3. Experimental

3.1. Isolation and purification of Ni DPEP

Isolation and purification of Ni DPEP were conducted according to the method described by Kashiyama et al. (2007), with slightly modified HPLC conditions. The pulverized sediments were Soxhlet extracted with chloroform/methanol (70:30, v/v) for ~72 h. The total lipid extracts were separated into seven fractions using silica gel column chromatography. Unwilling components other than Ni porphyrins concentrated in the third subfraction were removed by reversed phase open column chromatography prior to HPLC. Individual porphyrins, including Ni DPEP, were then isolated by a dual step HPLC (Kashiyama et al., 2007) to avoid chromatographic isotopic fractionation (Filer, 1999). In the first step separation in the reversed phase condition (described below), a fraction containing the entire peak of Ni DPEP was isolated (Fig. 3a). Here, co-eluting or closely eluting porphyrins were still contained in the fraction. Ni DPEP was then completely isolated from these impurities with *base line resolution* by the second step separation in the nor-

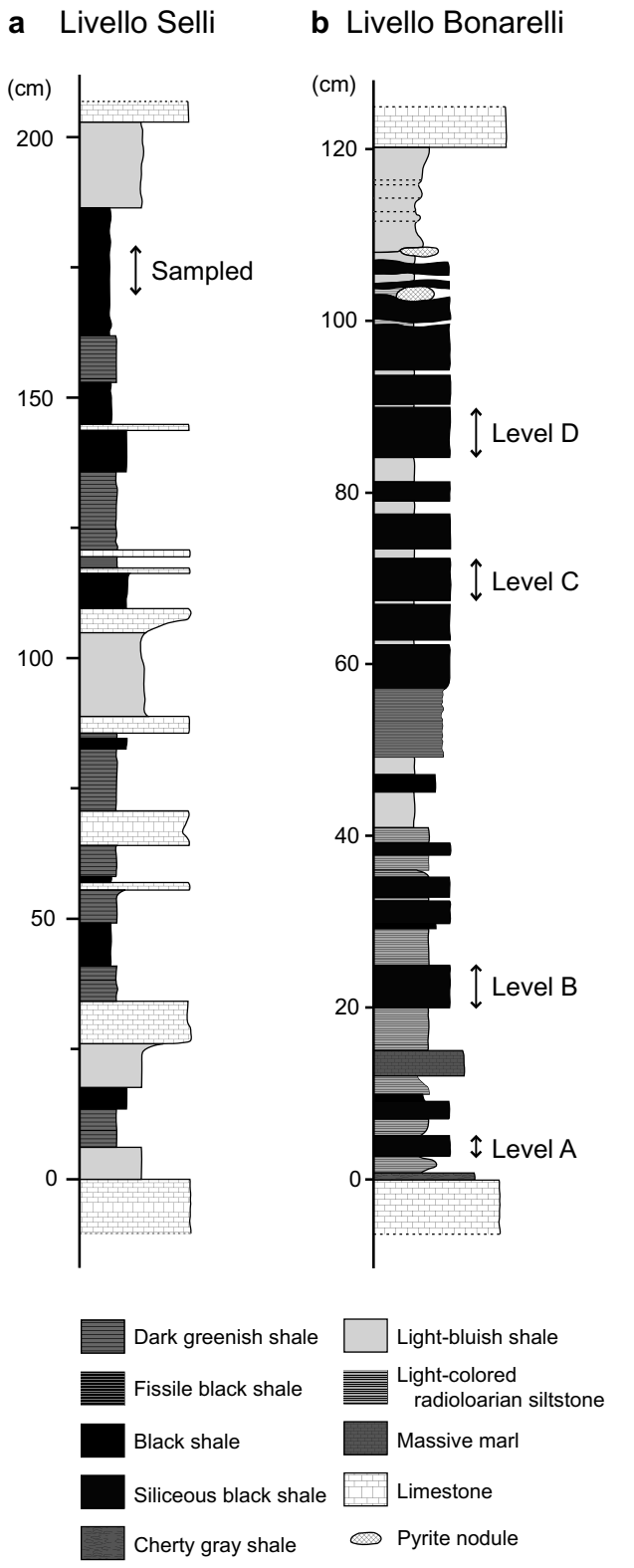

Fig. 2. Stratigraphic columns of (a) the Livello Selli black shale and (b) the Livello Bonarelli black shale at the Gorgo Cerbara section, Marche, Italy. Sedimentary porphyrins within black shale were analyzed at 172–178 cm from the base of the Livello Selli and from four discrete stratigraphic levels within the Livello Bonarelli: Level A: 2–5 cm, Level B: 20–25 cm, Level C: 67–72 cm, and Level D: 84–89 cm, as measured from the bottom of the shale.

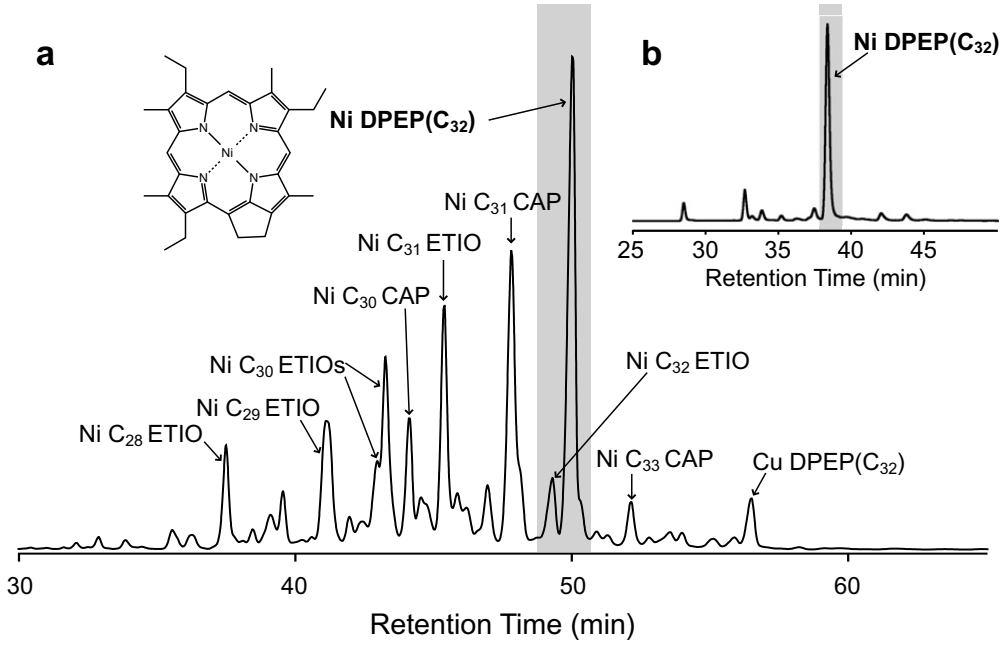

Fig. 3. Representative reversed and normal phase HPLC/DAD chromatograms (at 390 nm) of the Ni alkylporphyrins fraction (sample from the Livello Selli). (a) Reversed phase HPLC is the first step in the isolation of DPEP. The shaded fraction was collected and further separated by (b) normal phase HPLC, in which DPEP was separated from other porphyrins by base line resolution and collected for isotopic analysis (shaded fraction).

mal phase condition (Fig. 3b; described below). Kashiyama et al. (2007) demonstrated that such a fraction obtained after both reversed and normal phase HPLC does not contain any impurities other than co-eluting porphyrins, as based on observations using an evaporative light scattering detector (ELSD; Polymer Laboratories, PL-ELS 2100).

The purity of the isolated Ni DPEP was assessed in both HPLC chromatograms and NMR spectrum. Based on the area of the absorption chromatogram (at 392 nm), the purity of the isolated Ni DPEP was estimated to be better than 98%. Furthermore, an ^{1}H NMR spectrum of the isotopically analyzed Ni DPEP was clean, demonstrating the absence of any impurities (Fig. 4).

The HPLC system (Agilent 1100 series) comprised a binary pump, on-line degasser, autosampler, total temperature controller for HPLC columns (i.e., column oven; Selerity Technologies Inc.; The POLARATHERM™ Series 9000), and an on line photodiode array detector (DAD), as well as being optionally equipped with a fraction collector and a mass selective detector (MSD) connected via an atmospheric pressure chemical ionization (APCI) interface. The system was coupled to a personal computer on which Agilent Chemstation software was installed.

In the reversed phase HPLC, the analyses were performed using three analytical scale columns (ZORBAX SB-C18, 4.6 × 250 mm; 5 μm silica particle size) connected in series with a guard column (ZORBAX SB-C18, 4.6 × 12.5 mm; 5 μm silica particle size) set in front. The isocratic mobile phases were acetonitrile/water/acetic acid/pyridine (95:5:0.5:0.5, v/v). The column oven temperature program and flow rate are summarized in Table 1a. In the normal phase HPLC, analyses were performed using five analytical scale columns (ZORBAX Sil, 4.6 × 250 mm; 5 μm silica particle size) connected in series with a guard column (ZORBAX Sil, 4.6 × 12.5 mm; 5 μm silica particle size) set in front. The isocratic mobile phases were *n*-hexane/acetone/acetic acid/pyridine (97:3:0.5:0.5, v/v), and the flow rate was 1 ml min^{-1}. The column oven temperature program in the normal phase HPLC is summarized in Table 1b.

3.2. Identification of chemical structure

Ni DPEP was identified conclusively from chromatographic analysis with reference to our DPEP standard. The standard was originally obtained as VO complex from the middle Miocene Onnagawa Formation (Kashiyama, 2006) and structurally

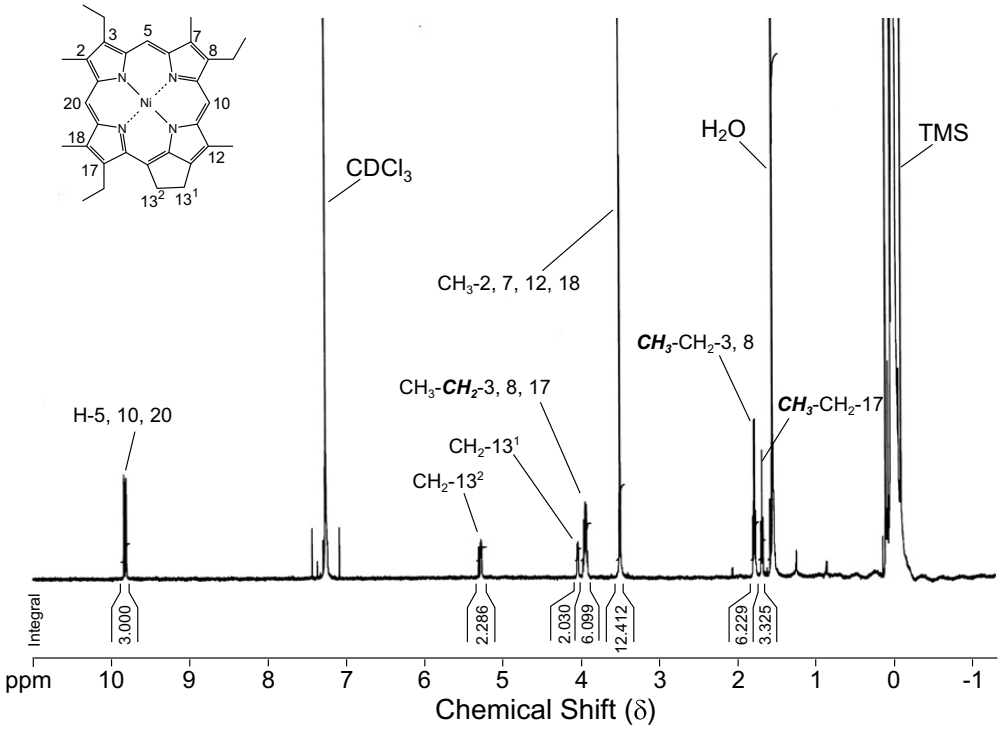

Fig. 4. Six hundred megahertz ^{1}H NMR spectrum of DPEP isolated as in Fig. 3 and used for isotopic analysis (dissolved in $CDCl_3$ with TMS).

determined by X-ray crystallography (Fig. 5)[1] before being transmetallated as Ni complex. The structures of other porphyrins (Fig. 3a) were temporarily estimated based on mass spectra, UV–Vis spectrum, and relative retention time. Identification was well supported by the ^{1}H NMR spectrum of DPEP isolated from the present samples (Fig. 4).

3.3. Isotopic analyses

Nitrogen and carbon isotopic compositions were determined by ThermoFinnigan Delta plus XP isotope-ratio mass spectrometry coupled to a Flash EA1112 automatic elemental analyzer via a Conflo III interface (EA/IRMS; Ohkouchi et al., 2005). Nitrogen and carbon isotopic compositions are expressed as conventional δ-notation. Isotopic compositions were calibrated against a laboratory standard compound with known isotopic compositions of $\delta^{15}N = +0.86‰$ and $\delta^{13}C = -34.17‰$ (Ni etioporphyrin I; Aldrich Chemical Co., Milwaukee, WI, USA).

The purified Ni DPEP and Ni etioporphyrin I standard were dissolved in chloroform and placed onto pre-cleaned tin capsules. After chloroform was evaporated, the capsules were carefully folded with forceps prior to analysis. Various quantities of the Ni etioporphyrin I standard were analyzed interspersed with the samples. The analytical precision of the isotopic compositions attributable to instrumental conditions were estimated to be 0.24–0.34‰ for nitrogen and 0.16–0.44‰ for carbon (2σ; ranges reflect the precision determined on different days). Analytical errors associated with the separation and purification procedures were assessed by repeating the procedures for triplicate samples from Level D of the Livello Bonarelli. The standard deviations of the three independent experiments were 0.82‰ for $\delta^{15}N$ and 0.20‰ for $\delta^{13}C$ (2σ). Thus, the inclusive analytical errors for

[1] Crystal data for vanadyl DPEP: $C_{33}H_{35}C_{l3}N_4OV$, fw 660.97, monoclinic, space group $P2_1/c$ (#14), $a = 12.7744(9)$Å, $b = 14.0984(8)$Å, $c = 18.1511(11)$Å, $\beta = 110.1851(16)°$, $V = 3068.2(3)$Å^3, $Z = 4$, MoKα radiation ($\lambda = 0.71075$Å), $D_{calc} = 1.431$ g cm^{-3}, μ(MoKα) = 6.182 cm^{-1}, 43060 measured reflections, 6954 unique reflections [$R_{int} = 0.090$], 6954 reflections included in the refinement, $R = 0.0671$ [$I > 2\sigma(I)$], $wR = 0.2054$ (all reflections). Crystallographic data for the structural analysis of vanadyl DPEP has been deposited with the Cambridge Crystallographic Data Centre (CCDC No. 652174). Copies of this information can be obtained free of charge from www.ccdc.cam.ac.uk.

Table 1
Gradient programs for column oven temperature and flow rate

(a) Reversed-phase HPLC			(b) Normal-phase HPLC		
Time (min)	Temperature (°C)	Flow rate (ml/min)	Time (min)	Temperature (°C)	Flow rate (ml/min)
0	40	1.0	0	35	1.0
10	40	1.0	10	35	1.0
50	80	1.8	60	45	1.0
60	80	1.8	70	45	1.0

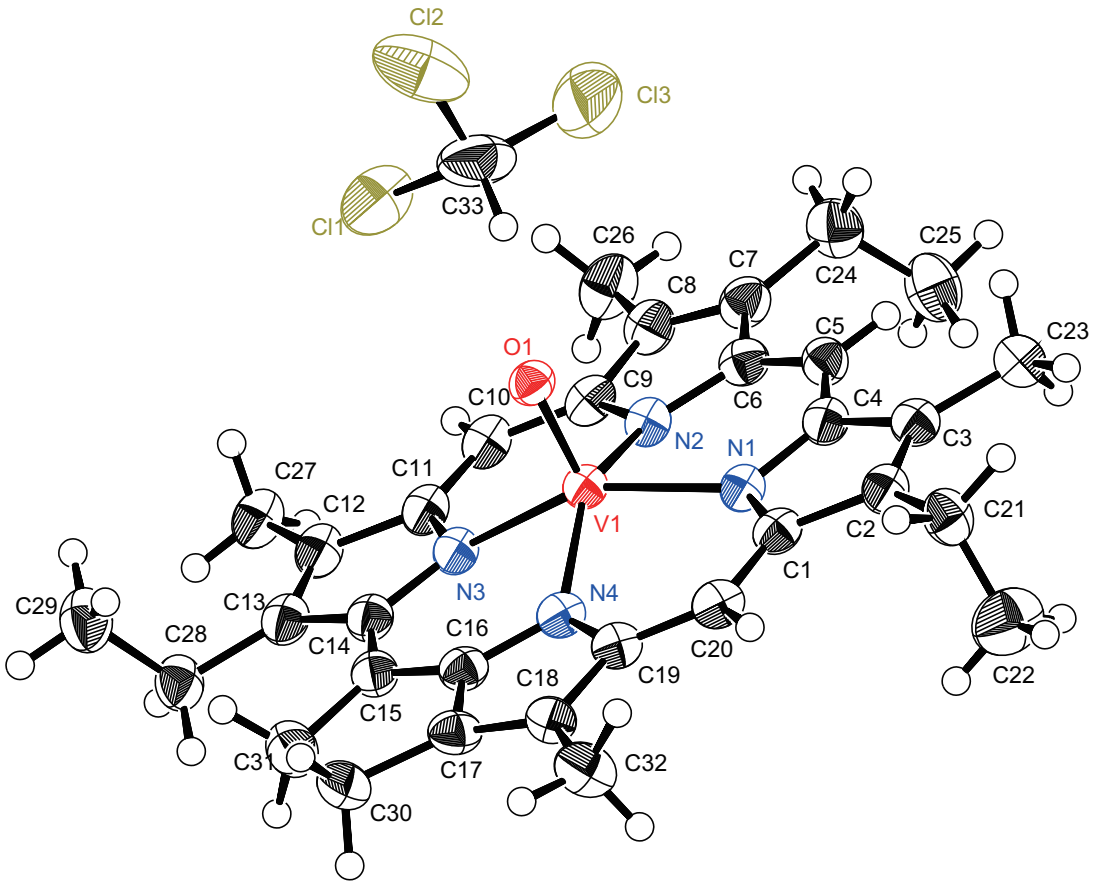

Fig. 5. X-ray crystal structure of vanadyl DPEP. Dark red block crystals of $C_{30}H_{30}N_4OV$ were grown by vapor diffusion (methanol into $CHCl_3$ solution). A single crystal with the approximate dimensions of $0.15 \times 0.12 \times 0.07$ mm was then mounted on a glass fiber. Measurements were made on a Rigaku RAXIS RAPID imaging plate area detector using graphite monochromated Cu Kα radiation.

the obtained data were 0.8‰ for nitrogen and 0.4‰ for carbon (2σ).

The standards employed for nitrogen and carbon were atmospheric N_2 (AIR) and the Peedee Belemnite (PDB), respectively. In the present work, we define isotopic fractionation between the substrate and product (ε) as follows:

$$\epsilon\ (‰) \equiv 10^3[(\delta_{\text{substrate}} + 1000)/(\delta_{\text{product}} + 1000) - 1]$$
$$\approx \delta_{\text{substrate}} - \delta_{\text{product}}$$

4. Results and discussion

4.1. Nitrogen and carbon isotopic compositions of Ni DPEP

Fig. 3 shows a representative chromatogram of reversed phase HPLC for the nickel porphyrin fraction. The major components do not differ among all samples of the Livello Selli and Livello Bonarelli black shales, but they do vary in their relative amounts. Ni DPEP (C_{32}) is the most abundant

nickel porphyrin in all of the analyzed samples (15–20% of the total nickel porphyrins), and C_{31} cycloalkanoporphyrin (CAP) is the second most abundant. Other major components, in general descending order of abundance, included C_{31} etioporphyrin type porphyrins (ETIO; i.e., no cycloalkano side chain), C_{30} CAP, two varieties of C_{30} ETIO, C_{29} ETIO, C_{28} ETIO, C_{32} ETIO, and C_{33} CAP.

Table 2 summarizes the carbon and nitrogen isotopic compositions of the isolated Ni DPEP from the analyzed samples of black shale. The nitrogen isotopic composition of the Ni DPEP showed characteristically negative $\delta^{15}N$ values, ranging from −6.6‰ to −3.9‰. A systematic trend is observed in the $\delta^{13}C$ values of Ni DPEP among the four stratigraphic levels of the Livello Bonarelli: $\delta^{13}C$ is most strongly negative at the base (−20.5‰; Level A), showing an upward increase of nearly 3‰ to Level D. This trend correlates exactly with the positive excursion observed for the $\delta^{13}C$ values of bulk organic matter in this section (Kuroda et al., 2007; Fig. 6), probably recording a global $\delta^{13}C$ variation due to the enhanced burial rate of ^{13}C depleted organic carbon during OAE-2 (Kuroda et al., 2007).

4.2. Estimates of carbon and nitrogen isotopic compositions of paleo-photoautotrophs

We reconstructed the mean $\delta^{15}N$ and $\delta^{13}C$ values of the entire photoautotrophic community, which we assumed to be represented by Ni DPEP, based on the isotopic differences empirically observed between the tetrapyrrole nuclei of chlorophylls and the whole cell organic matter reported elsewhere (Ohkouchi et al., 2006, 2007). Because the tetrapyrrole nuclei were synthesized via a unique biosynthetic pathway in all photoautotrophs after condensation of eight molecules of 5-aminolevulinic acid (ALA; Beale, 1995), relatively simple isotopic relationships were expected between the cells of photoautotrophs and chlorophylls, and hence between paleo-photoautotrophs and DPEP.

Table 2
Nitrogen and carbon isotopic compositions of Ni DPEP

	$\delta^{15}N$ (‰)	$\delta^{13}C$ (‰)
Livello Selli	−3.9	−18.9
Livello Bonarelli		
Level A	−4.9	−20.5
Level B	−5.6	−19.6
Level C	−6.6	−17.9
Level D	−5.5	−18.0

As concluded by Ohkouchi et al. (2006), the tetrapyrrole nuclei are depleted in ^{15}N by 4.8 ± 1.4‰ (1σ, $n = 20$) relative to the cell, reflecting intermolecular nitrogen transfer along the synthesis of ALA from glutamate catalyzed by glutamate-1-semialdehyde aminotransferase (Mau and Wang, 1988; Mayer et al., 1993). In contrast, the $\delta^{13}C$ value of the tetrapyrrole nuclei is enriched in ^{13}C by 1.8 ± 0.8‰ (1σ, $n = 18$) relative to the cell (Ohkouchi et al., 2007). The isotopic composition of the tetrapyrrole nuclei is expected to be preserved after diagenetic modification before being preserved as DPEP. Thus, we conclude that DPEP is depleted in ^{15}N by approximately 4.8‰ and enriched in ^{13}C by approximately 1.8‰ relative to its source photoautotrophs in the paleo-ocean. Fig. 7 shows the reconstructed mean isotopic compositions of carbon and nitrogen for the entire photoautotrophic community. Characteristically low values of $\delta^{15}N$ for the entire community are estimated from the low values of Ni DPEP for all of the horizons within the Livello Bonarelli (−2‰ to 0‰) and Livello Selli (+0.9‰).

4.3. Biogeochemical significance of nitrogen isotopic composition

The estimated $\delta^{15}N$ values are substantially lower than those observed for common photoautotrophic communities in modern oceans in which nitrate is the major substrate for new photoautotrophic production. Because nitrate is generally used up in the surface ocean, the $\delta^{15}N$ value of the photoautotrophic cell largely reflects that of nitrate. In the modern subsurface ocean, the nitrogen isotopic composition of nitrate ranges from +5‰ to +7‰, but may reach ~+13‰ in regions of upwelling (Miyake and Wada, 1967; Liu and Kaplan, 1989; Sigman et al., 2000; Sutka et al., 2004). These elevated $\delta^{15}N$ values in oceanic water are attributed to biological denitrification that selectively removes $^{14}NO_3^-$ as N_2 or N_2O (Cline and Kaplan, 1975; Liu and Kaplan, 1989; Brandes et al., 1998; Altabet et al., 1999; Barford et al., 1999; Voss et al., 2001; Sigman et al., 2003). In practice, the $\delta^{15}N$ values of POM from surface water range from, for example, +3‰ to +8‰ in the southwest Indian Ocean (Altabet and Francois, 1994) and from +4‰ to +16‰ in the upwelling region of the eastern tropical Pacific (Saino and Hattori, 1987; Altabet et al.,

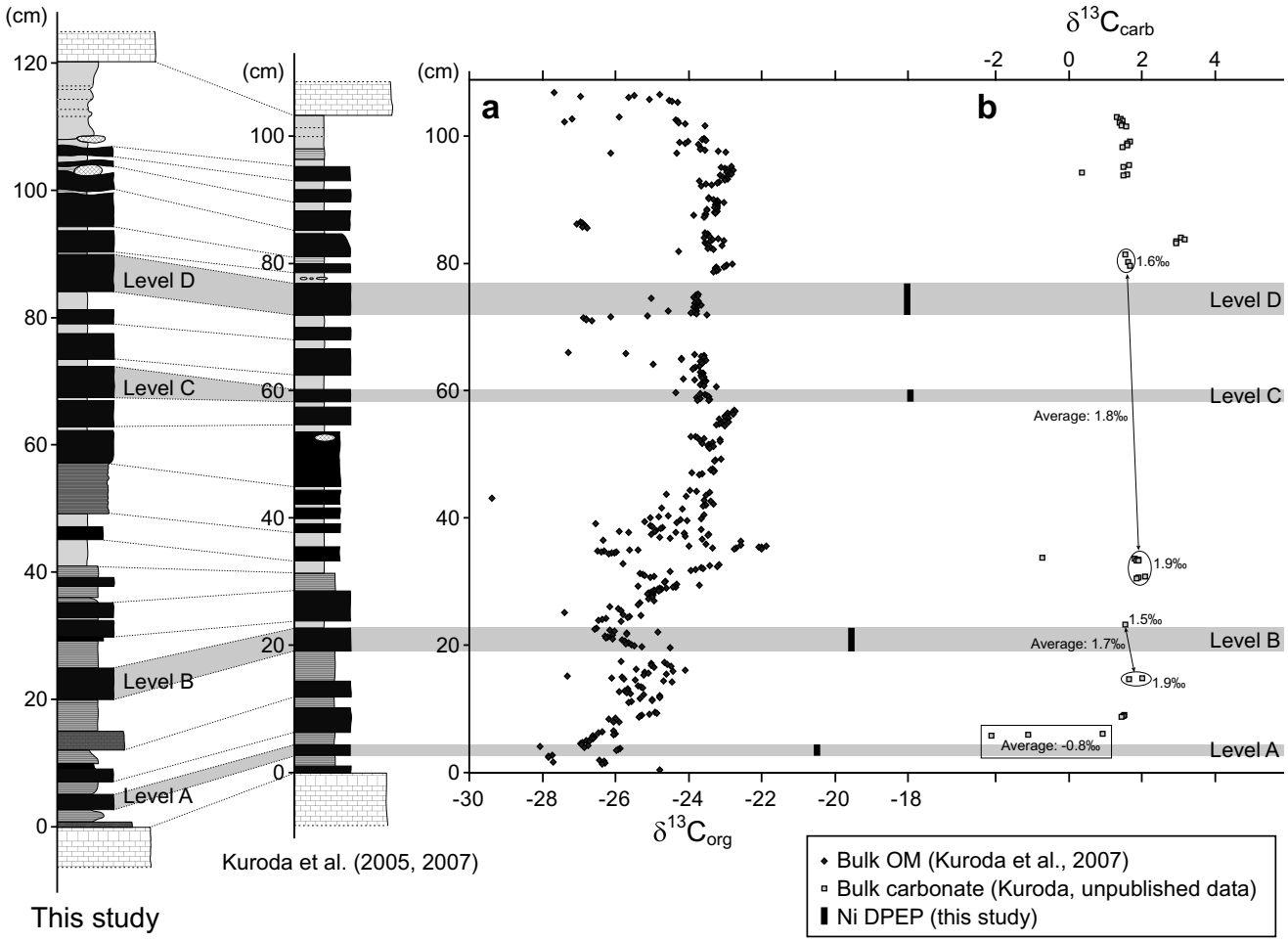

Fig. 6. Stratigraphic column of the Livello Bonarelli black shale at the Gorgo Cerbara section based on data from the present study and Kuroda et al. (2005), showing Kuroda et al. (2005) $\delta^{13}C$ data for (a) bulk organic matter and (b) bulk carbonate. (For interpretation of the references to colour in this figure legend, the reader is referred to the web version of this article.)

1999; Voss et al., 2001). Therefore, our low $\delta^{15}N$ value for photoautotrophs (−2‰ to +1‰) cannot be explained in this context unless unusually low $\delta^{15}N$ values of nitrate (~0‰) are assumed.

To explain the low $\delta^{15}N$ values recorded in the present study, we considered the following two possibilities. First, we explored the possibility of nitrate assimilation under excess nitrate surface water, which could occur when photoautotrophic production is limited by factors other than nitrate availability. Isotopic fractionation associated with nitrate uptake ($\varepsilon = -10$ to -4; Wada and Hattori, 1978; Waser et al., 1998; Needoba et al., 2003) may have resulted in a significant depletion of ^{15}N for photoautotrophic cells relative to the substrate (e.g., ~+6‰ in the modern ocean). In such a case, the $\delta^{15}N$ value of photoautotrophic cells would potentially lie in the range recorded for the Livello Selli and the Livello Bonarelli (−2‰ to +1‰).

Second, we considered N_2 fixation as the source of nitrogen for new production, as observed in nitrate deficient oligotrophic water in the modern ocean. In detail, the nitrogen introduced to the net photosynthetic system in the oligotrophic ocean is derived mainly from N_2 fixers, which results in mean $\delta^{15}N$ values of photoautotrophs ranging from −2‰ to 0‰. These values overlap exactly with the range of estimated $\delta^{15}N$ values for the entire photoautotrophic community of the Livello Bonarelli (−2‰ to 0‰) and are similar to the value obtained for the Livello Selli (~+1‰).

If the second scenario was indeed the case, there are two reasons to suggest that the major diazotrophs could have been cyanobacteria: (1) the quantitatively significant precursor of DPEP is expected to be chlorophyll *a*, the *major* antenna pigment of virtually all oxygenic photoautotrophs; and (2) among diazotrophic photoautotrophs, only

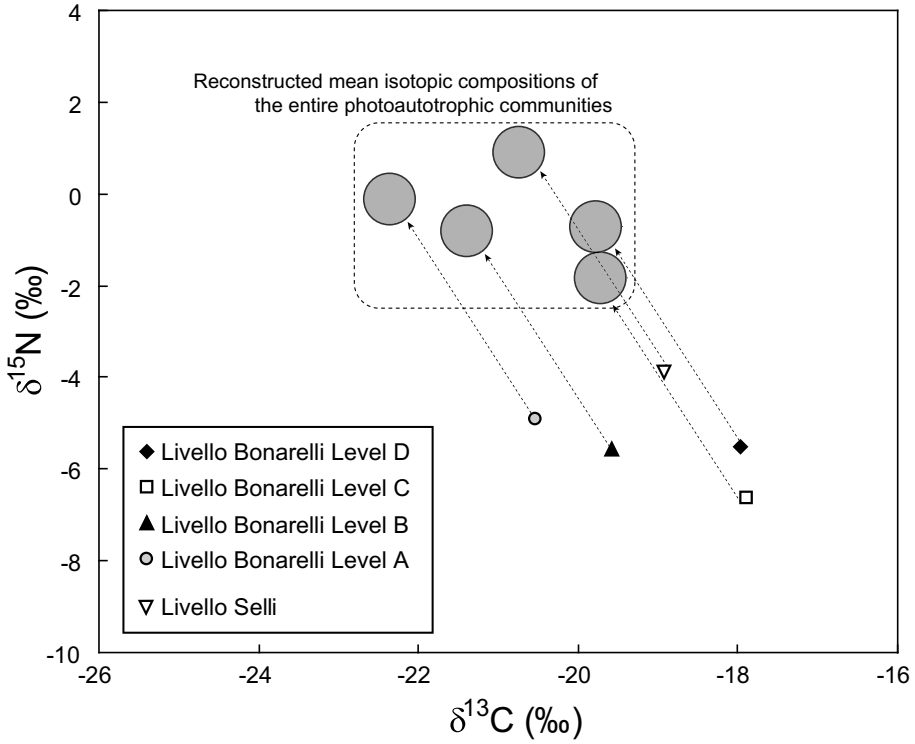

Fig. 7. Reconstructed $\delta^{15}N$ and $\delta^{13}C$ values for photoautotrophic cells within the Livello Selli and Livello Bonarelli black shales. Shaded circles represent the approximate ranges of the mean isotopic compositions for the photoautotrophic community, as reconstructed from Ni DPEP for each stratigraphic level.

cyanobacteria inhabit aerobic environments and synthesize chlorophyll *a*. Indeed, the bloom forming diazotrophic cyanobacteria *Trichodesmium* are major primary producers in many areas of the modern oligotrophic ocean, where they contribute to the supply of new nitrogen in the surface water (Capone et al., 1997, 2005; Carpenter et al., 1997; Karl et al., 1997; Davis and McGillicuddy, 2006). Diazotrophic unicellular cyanobacteria have also been reported in the oligotrophic ocean, potentially contributing to the nitrogen cycle in this environment (Zehr et al., 2001; Montoya et al., 2004).

4.4. Biogeochemical significance of carbon isotopic composition

Further constraints on the physiology of photoautotrophs can be inferred from the carbon isotopic composition of sedimentary porphyrins. Based on the $\delta^{13}C$ values of DPEP, we estimated the $\delta^{13}C$ values of the photoautotrophic biomass in the western Tethys Sea to have been approximately −21‰ during OAE-1a and between −22‰ and −20‰ during OAE-2. A 3‰ positive shift in the $\delta^{13}C$ values of the photoautotrophic biomass was observed in the lower level of the Livello Bonarelli black shale (Fig. 6), mirroring the observed trends in bulk organic matter, carbonates (Fig. 6), and other biomarkers (Kuroda et al., 2007), and hence presumably recording the 3‰ positive shift in the $\delta^{13}C$ values of dissolved inorganic carbon. The observed positive shift records the recovery from the abrupt negative shift at the base of the black shale within the "maximum plateau phase" of OAE-2 (Kuroda et al., 2007). Regardless of the isotopic perturbations of the carbon substrate, the estimated values of overall isotopic fractionation during photosynthesis (ε_p values) show only minor variation within the Livello Bonarelli black shale (Table 3).

In addition to the present data, Pancost et al. (2004) reported a $\delta^{13}C$ profile for methyl ethyl maleimide – a decomposed product of chlorophylls/porphyrins – from the Livello Bonarelli black shale of the Monte Petrano section, located just 10 km southeast of the Gorgo Cerbara section analyzed in the present study. Ohkouchi et al. (2007) suggested that alkyl maleimides from geological samples should be somewhat depleted in ^{13}C relative to porphyrins because the carbons at the methine bridges of porphyrin structure removed in the course of maleimide generation tend to be enriched in ^{13}C relative to the rest of the carbons in the structure.

Table 3
Observed and estimated values of various carbon isotopic terms

	δ_{DPEP} (‰) (observed)	δ_{cell} (‰) (estimated[1])	δ_c (‰) (observed)	δ_d (‰) (estimated[2])	ε_p (‰) (estimated[3])
Livello Selli	−18.9	−21	4	−5 ~ −4	−16 ~ −17
Livello Bonarelli					
Level A	−20.5	−22	−0.8	−9	−13 ~ −14
Level B	−19.6	−21	1.7	−7 ~ −6	−15
Level C	−17.9	−20	1.8	−7 ~ −6	−13 ~ −14
Level D	−18.0	−20	1.6	−7 ~ −6	−13 ~ −14

In calculating the ε_p values, the $\delta^{13}C$ value of CO_2(aq) (δ_d) was estimated based on that of carbonates (δ_c). The δ_c values for the Livello Bonarelli were estimated from carbonates sampled from the same sections (Fig. 6). Given that the sampling level of the Livello Selli is devoid of carbonate, we adopted the δ_c value of 4‰ obtained from the limestone immediately above the Livello Selli at the same locality. The equilibrium isotopic discriminations between CO_3^{2-} and HCO_3^- ($\varepsilon_{b/c}$) and between HCO_3^- and CO_2(aq) ($\varepsilon_{d/b}$) were calculated based on the relationships determined by Thode et al. (1965) and Mook et al. (1974). We considered wide ranges for estimates of sea surface temperature, ~26 (±4) °C and ~30 (±4) °C for OAE-1a and OAE-2, respectively (Schouten et al., 2003; Jenkyns et al., 2004; Forster et al., 2007), and sea surface salinity of 34‰.

1: $\delta_{cell} = \delta_{DPEP} - 1.8$ (‰).

2: $\delta_d = \delta_c + (\delta_{b/c} + \delta_{d/b}) = \delta_c + ([653.627/(T - 233.45)^2] + 0.22) + (24.12 - 9866/T)$ (‰); after Thode et al. (1965) and Mook et al. (1974).

3: $\varepsilon_p = \delta_{cell} - \delta_d$ (‰).

In this context, the $\delta^{13}C$ values of maleimide reported by Pancost et al. (2004) (−23‰ to −20‰) are largely consistent with our $\delta^{13}C$ data for DPEP (−21‰ to −18‰).

Analyses of porphyrins as well as phytane and pristane from other basins reveal relatively negative $\delta^{13}C$ values for the photoautotrophic biomass during background intervals prior to and following Cretaceous OAEs (Hayes et al., 1989, 1990; Kuypers et al., 1999, 2001, 2004). In fact, this line of evidence is the main theoretical basis for interpretations of elevated P_{CO_2} during the Cretaceous (e.g., Dean et al., 1986; Popp et al., 1989; Freeman and Hayes, 1992; Tajika, 1998). In particular, Kuypers et al. (1999, 2002, 2004) reported the $\delta^{13}C$ values of sulfur bound phytane (~−30‰) from immediately below OAE-2 black shales in North Atlantic sites. The sulfur bound phytane was presumably derived from the phytyl group of chlorophylls (Kohnen et al., 1992). Because the phytyl group is depleted in ^{13}C by approximately 4 ± 1.9‰ ($n = 18$) relative to the cell (Ohkouchi et al., 2007), the $\delta^{13}C$ value of the photoautotrophic biomass was estimated to be ~−26‰. Similar estimates have been obtained for pre- and post-OAE-2 sediments of the Western Interior Seaway (the Greenhorn Formation), based on both the isotopic analyses of total nickel porphyrins (Hayes et al., 1989) and derivatives of phytol (phytane and pristane; Hayes et al., 1990).

These previous workers all showed that during OAE-2, $\delta^{13}C$ values increased, typically to a greater extent than inorganic carbon records, such that estimated ε_p values decreased. Namely, $\delta^{13}C$ values of photoautotrophic biomass were raised up to −24‰ to −21‰ in the North Atlantic (estimated from $\delta^{13}C$ of sulfur bound phytane: −28‰ to −25‰; Kuypers et al., 1999, 2002, 2004) and −28‰ to −27‰ in the Western Interior Seaway (estimated from $\delta^{13}C$ of nickel porphyrins: −26‰ to −25‰; Hayes et al., 1989). This has been attributed to either lower P_{CO_2} levels (Arthur et al., 1988; Freeman and Hayes, 1992) and/or increased algal growth rates (Kuypers et al., 2002).

We observed even higher $\delta^{13}C$ values for photoautotrophic biomass in the western Tethys Sea (−22‰ to −20‰) compared to these previous studies (−28‰ to −21‰). This suggests significantly lower ε_p values in the western Tethys Sea relative to other geographical sites. A reduced ε_p value can be attributed to environmental factors that control [CO_2(aq)], including atmospheric P_{CO_2} and sea surface temperature (SST), or physiological factors. Atmospheric P_{CO_2} is an unlikely explanation, because that would clearly affect all sites, regardless of geographical location. Lower ε_p values could be due to lower [CO_2(aq)] and therefore reflect elevated SST (Popp et al., 1989; Jasper and Hayes, 1990; Freeman and Hayes, 1992; Rau et al., 1992; Francois et al., 1993). However, to explain the 6–7‰ difference between our calculated ε_p values and those in the Western Interior Seaway, for example, Tethyan SSTs must have been >30 °C greater than those in the Western Interior Seaway. That is unlikely, and we suspect that the low ε_p values in the western Tethys Sea were caused mainly by the physiological

characteristics of the photoautotrophs rather than [CO_2(aq)].

It has been well demonstrated that elevated growth rates of photoautotrophs result in lower ε_p values (e.g., Bidigare et al., 1997; Pancost et al., 2004). The ε_p values estimated in the present study for the western Tethys Sea (13–17‰; Table 3) are in fact comparable to values observed under the present day low P_{CO_2} conditions (Bidigare et al., 1997,1999). Under the elevated P_{CO_2} setting of the mid-Cretaceous (Freeman and Hayes, 1992; Tajika, 1998), explanation of the observed anomaly requires an exceptionally high growth rate of photoautotrophs, which should be comparable to those observed in areas of strong upwelling (e.g., the modern Peru margin; Bidigare et al., 1997).

Alternatively, the observed anomaly could be explained by the effects of specific biogeochemical processes that may have been characteristic of particular taxa. Lower ε_f values could have resulted from the presence of phosphoenolpyruvate carboxylase (PEPC), an alternative carboxylation enzyme (i.e., β-carboxylation; Descolas-Gros and Fontugne, 1985, 1990; Raven, 1997). In carboxylation by PEPC, ^{13}C enriched bicarbonate ion is used as a substrate; consequently, the apparent isotopic fractionation (relative to CO_2(aq)) is as low as ~5‰ (e.g., Smith and Epstein, 1971; O'Leary et al., 1992). The lower ε_p values could also have resulted from enzymatically catalyzed active transport of $CO_2(aq)/HCO_3^-$ into the cell (Sharkey and Berry, 1985; Fogel and Cifuentes, 1993; Goericke et al., 1994; Hinga et al., 1994; Pancost et al., 1997; Raven, 1997).

4.5. Paleoecology of the prevailing photoautotrophs

Here, we demonstrate that the combined evidence of the estimated nitrogen and carbon isotopic compositions of photoautotrophs constrains the characteristics of their unique ecology and physiology, which are potentially related to the deposition of organic rich black shales during OAEs. Specifically, we infer that diazotrophic cyanobacteria were the dominant primary producers during OAE-1a and OAE-2 in the western Tethys Sea.

The nature of the nitrogen isotopic record points to two mutually exclusive environments: nitrate assimilation in excess nitrate surface water and N_2 fixation in nitrate deficient surface water. The former condition is incompatible with the lower ε_p values estimated based on the $\delta^{13}C$ values of Ni DPEP, as photoautotrophic production in excess nitrate surface water in the modern ocean is characterized by significantly higher ε_p values. For example, the modern Southern Ocean to the south of the polar front zone (55–65°S) is a region with excess nitrate in the surface water, and the ε_p value associated with photosynthesis is higher than that observed at lower latitudes, partially because of the ecological requirements of photoautotrophs under these conditions (Popp et al., 1998,1999). This is in contrast with the cases for the Livello Selli and Livello Bonarelli, for which the magnitude of isotopic fractionation (ε_p) is lower than that expected for a high P_{CO_2} world. Thus, we conclude that during both OAE-1a and OAE-2 in the western Tethys Sea, the nitrogen utilized by the photoautotrophic community was supplied mostly via N_2 fixation by cyanobacteria.

Meanwhile, the lower ε_p values obtained in the present study suggested either a highly elevated growth rate of photoautotrophs that is expected in upwelling center or a physiological expression of photoautotrophs resulting in a diminished ε_f value. The former does not agree with the evidence from the nitrogen, however, because biomass produced in the upwelling center should generally have a relatively elevated $\delta^{15}N$ value reflecting ^{15}N enriched nitrate supplied from the deep water. On the other hand, the latter possibility is indeed concordant to the suggestion from nitrogen isotopic compositions that cyanobacteria were the major photoautotrophs during the mid-Cretaceous. Previous reports state that the $\delta^{13}C$ values of field collected *Trichodesmium*, a bloom forming marine cyanobacterium, tend to be lower, probably as a result of relatively minor isotopic fractionation during CO_2 uptake (Calder and Parker, 1973; Wada and Hattori, 1991; Carpenter et al., 1997). In an unusual case, Carpenter et al. (1997) reported $\delta^{13}C$ values of -12.9 ± 1.1‰ (1σ, $n = 10$) for *Trichodesmium* cells from the southeast North Atlantic and the northwestern Caribbean Sea within stratified oligotrophic surface water, indicating a ε_p value of >-10‰. Such an apparently small degree of isotopic fractionation suggests β-carboxylation by PEPC and/or active transport of the carbon substrate, which would have fueled their rapid growth in generating blooms.

PEPC is known to be an important carboxylation enzyme for cyanobacteria (Colman, 1989; Tabita, 1993). Sakata et al. (1997) reported that the tetrapyrrole nuclei of chlorophyll *a* within the cyanobacterium *Synechocystis* was 2.7‰ enriched in ^{13}C

relative to the cell, which is larger than the value we proposed in the present study. In explaining this enrichment, the authors suggested that the synthesis of oxaloacetate (a precursor of glutamate in the TCA cycle) from the β-carboxylation of phosphoenolpyruvate by PEPC results in ^{13}C enriched glutamate, and thus ^{13}C enriched tetrapyrrole nuclei. If carboxylation by PEPC was an important process during the mid-Cretaceous, our estimate of the $\delta^{13}C$ values of the photoautotrophs could be somewhat lower than the actual $\delta^{13}C$ values; hence, the actual ε_p values are lower than the *apparent* estimate. Even if the actual ε_p values were a few per mil higher, they are still lower than the expected values for ordinary photosynthesis. Thus, PEPC related β-carboxylation by cyanobacteria could potentially have had the following dual effects that contributed to the apparently lower ε_p values: (1) the synthesis of relatively ^{13}C enriched tetrapyrrole nuclei of chlorophylls, and (2) a reduction in the overall degree of carbon isotopic fractionation.

Moreover, cyanobacteria commonly adopt the active transport of $CO_2(aq)/HCO_3^-$ to elevate intracellular $[CO_2(aq)]$, thereby compensating for the low affinity of the Rubisco of cyanobacteria for CO_2 (Kaplan et al., 1980; Ogawa, 1993; Kaplan and Reinhold, 1999; Badger and Spalding, 2000; Ogawa and Kaplan, 2003); however, it is not clear to what degree the active transport and β-carboxylation contribute to the carbon assimilation of cyanobacteria in the natural environment. Greater understanding in this regard is required to make more detailed interpretations based on the available carbon isotopic evidence.

5. Conclusions and implications

We estimate that the mean nitrogen isotopic compositions of the entire photoautotrophic communities in the western Tethys Sea during OAE-1a and OAE-2 were in the range from −2‰ to +1‰. This finding suggests that the nitrogen assimilated during the new production of photoautotrophs was either supplied by nitrate in excess nitrate surface water or N_2 fixation by diazotrophic cyanobacteria in nitrate deficient surface water. The estimated mean $\delta^{13}C$ values of the entire photoautotrophic communities during both OAEs were relatively elevated compared to other sites, indicating reduced carbon isotopic fractionation during carboxylation by photoautotrophs in the western Tethys Sea. The obtained values are significantly lower than those expected under normal photoautotrophic physiological conditions assuming Rubisco carboxylation and the diffusion of $CO_2(aq)$ substrate into the cells. Such a small degree of carbon isotopic fractionation is incompatible with photoautotrophic growth in excess nitrate environments; however, it is compatible with cyanobacterial primary production, whereby β-carboxylation and/or active transport of the carbon substrates could have resulted in the observed diminished degree of carbon isotopic fractionation.

The importance of cyanobacteria in primary production has also been reported from the North Atlantic. Kuypers et al. (2004) reported elevated concentration of 2-methyl hopanoids, the biomarker specifically derived from membrane lipids of cyanobacteria, from both OAE-1a and OAE-2 of the North Atlantic as well as western Tethys sites, suggesting the substantial contribution of pelagic cyanobacteria. In contrast, we did not observe 2-methyl hopanoids in the Livello Selli and Livello Bonarelli black shales. We suspect that the cyanobacteria that dominated primary production in the western Tethys Sea could have lacked 2-methyl hopanoids, as these lipids have only been reported from about half of the cyanobacterial species investigated to date (Summons et al., 1999).

The dominance of diazotrophic cyanobacteria as primary producers strongly suggests the occurrence of nitrate deficient oligotrophic surface water, because cyanobacteria conduct energetically expensive N_2 fixation when nitrate is deficient in the ambient water. A likely oceanographic condition in this regard is stratification of the water column, which acts to suppress the supply of nutrients from deep water to the surface. In the modern ocean, diazotrophic cyanobacteria primarily inhabit the upper euphotic zone in the stratified oligotrophic oceans of tropical and subtropical regions, occasionally forming extensive blooms (e.g., Marumo and Asaoka, 1974; Carpenter and McCarthy, 1975; Carpenter, 1983; Carpenter and Romans, 1991; Capone et al., 1997; Dupouy et al., 2000; Capone et al., 2005).

The results of the present study clarified the fact that the production of diazotrophic cyanobacteria (and possibly the production of algae supported by nitrogen supplied from the diazotrophic cyanobacteria) contributed to the sequestration of atmospheric CO_2 into the studied black shale, although further studies at other sites are required to gain a full understanding of the mid-Cretaceous OAEs.

These OAEs can be viewed as global scale, catastrophic disturbances of biogeochemical cycles, especially of the carbon and nitrogen cycles. Photoautotrophic primary production plays a central role in this regard, driving these cycles by photochemical energy. An understanding of biogeochemical processes mediated by photoautotrophs is therefore of crucial importance; in this context, compound specific isotopic studies of sedimentary porphyrins represent a promising approach.

Acknowledgments

We thank E. Tajika, H. Kawahata, Y. Yokoyama, and Y. Chikaraishi for helpful discussions. We also thank R. Coccioni, M. Tejada, and T. Sakamoto for support in the field and H. Suga for technical support in the laboratory. We are deeply indebted to Dr. Richard Pancost and two anonymous reviewers for their critical reviews and advice. This study was financially supported by the COE Program at The University of Tokyo, JOGMEC, a Grant-in-Aid for Creative Scientific Research (19GS0211), and JSPS.

Associate Editor—**Rich Pancost**

References

Altabet, M.A., Pilskaln, C., Thunell, R., Pride, C., Sigman, D., Chavez, F., Francois, R., 1999. The nitrogen isotope biogeochemistry of sinking particles from the margin of the eastern North Pacific. Deep Sea Research, Part I 46, 655–679.

Altabet, M.A., Francois, R., 1994. Sedimentary nitrogen isotopic ratio as a recorder of surface ocean nitrate utilization. Global Biogeochemical Cycles 8, 103–116.

Arthur, M.A., Premoli Silva, I., 1982. Development of widespread organic carbon-rich strata in the Mediterranean Tethys. In: Schlanger, S.O., Cita, M.B. (Eds.), Nature and Origin of Cretaceous Carbon-Rich Facies. Academic Press, St. Louis, pp. 7–54.

Arthur, M.A., Sageman, B.B., 1994. Marine black shales: depositional mechanisms and environments of ancient deposits. Annual Review of Earth and Planetary Sciences 22, 499–551.

Arthur, M.A., Schlanger, S.O., Jenkyns, H.C., 1987. The Cenomanian-Turonian oceanic anoxic event, II. Palaeoceanographic controls on organic-matter production and preservation. In: Brooks, J., Fleet, A.J. (Eds.), Marine and Petroleum Source Rocks, vol. 26. Geological Society Special Publications, pp. 401–420.

Arthur, M.A., Dean, W.A., Pratt, L.M., 1988. Geochemical and climatic effects of increased marine organic carbon burial at the Cenomanian/Turonian boundary. Nature 335, 714–717.

Arthur, M.A., Brumsack, H.-J., Jenkyns, H.C., Schlanger, S.O., 1990. Stratigraphy, geochemistry, and paleoceanography of organic carbon-rich Cretaceous sequences. In: Ginsburg, R.N., Beaudoin, B. (Eds.), Cretaceous Resources, Events and Rhythms. Kluwer Academic Publishers., pp. 75–119.

Badger, M.R., Spalding, M.H., 2000. CO_2 acquisition, concentration and fixation in cyanobacteria and algae. In: Leegood, R.C., Sharkey, T.D., von Caemmerer, S. (Eds.), Advances in Photosynthesis, Photosynthesis: Physiology and Metabolism, vol. 9. Kluwer Academic Publishers, Dordrecht, pp. 399–434.

Baker, E.W., Louda, J.W., 1986. Porphyrins in the geological record. In: Johns, R.B. (Ed.), Biological Markers in Sediments. Methods in Geochemistry and Geophysics, vol. 24. Elsevier, Amsterdam, pp. 125–225.

Barford, C.C., Montoya, J.P., Altabet, M.A., Mitchell, R., 1999. Steady-state nitrogen isotope effects of N_2 and N_2O production in *Paracoccus denitrificans*. Applied and Environmental Microbiology 65, 989–994.

Beale, S.I., 1995. Biosynthesis and structures of porphyrins and heme. In: Blankenship, R.E., Madigan, M.T., Bauer, C.E. (Eds.), Anoxygenic Photosynthetic Bacteria. Kluwer Academic Publishers, Netherland, pp. 153–177.

Bidigare, R.R., Fluegge, A., Freeman, K.H., Hanson, K.L., Hayes, J.M., Hollander, D., Jasper, J.P., King, L.L., Laws, E.A., Milder, J., Millero, F.J., Pancost, R., Popp, B.N., Steinberg, P.A., Wakeham, S.G., 1997. Consistent fractionation of ^{13}C in nature and in the laboratory: Growth-rate effects in some haptophyte algae. Global Biogeochemical Cycles 11, 279–292.

Bidigare, R.R., Fluegge, A., Freeman, K.H., Hanson, K.L., Hayes, J.M., Hollander, D., Jasper, J.P., King, L.L., Laws, E.A., Milder, J., Millero, F.J., Pancost, R., Popp, B.N., Steinberg, P.A., Wakeham, S.G., 1999. Erratum: "Consistent fractionation of ^{13} C in nature and in the laboratory: Growth-rate effects in some haptophyte algae". Global Biogeochemical Cycles 13, 251–252.

Boreham, C.J., Fookes, C.J.R., Popp, B.N., Hayes, J.M., 1989. Origins of etioporphyrins in sediments: evidence from stable carbon isotopes. Geochimica et Cosmochimica Acta 53, 2451–2455.

Boreham, C.J., Fookes, C.J.R., Popp, B.N., Hayes, J.M., 1990. Origin of petroporphyrins. 2. Evidence from stable isotopes. Energy & Fuels 4, 658–661.

Brandes, J.A., Devol, A.H., Yoshinari, T., Jayakumar, D.A., Naqvi, S.W.A., 1998. Isotopic composition of nitrate in the central Arabian Sea and eastern tropical North Pacific: a tracer for mixing and nitrogen cycles. Limnology and Oceanography 43, 1680–1689.

Calder, J.A., Parker, P.L., 1973. Geochemical implications of induced changes in C^{13} fractionation by blue-green algae. Geochimica et Cosmochimica Acta 37, 133–140.

Callot, H.J., Ocampo, R., 2000. Geochemistry of porphyrins. In: Kadish, K.M., Smith, K.M., Guiland, R. (Eds.), The Porphyrin Handbook, Synthetic and Organic Chemistry, vol. 1. Academic Press, New York, pp. 349–398 (Chapter 7).

Capone, D.G., Zehr, J., Paerl, H., Bergman, B., Carpenter, E.J., 1997. *Trichodesmium*: A globally significant marine cyanobacterium. Science 276, 1221–1229.

Capone, D.G., Burns, J.A., Montoya, J.P., Subramaniam, A., Mahaffey, C., Gunderson, T., Michaels, A.F., Carpenter, E.J., 2005. Nitrogen fixation by *Trichodesmium* spp.: An important source of new nitrogen to the tropical and subtropical North Atlantic Ocean. Global Biogeochemical Cycles 19, GB2024.

Carpenter, E.J., 1983. Physiology and ecology of marine planktonic *Oscillatoria* (*Trichodesmium*). Marine Biology Letters 4, 69–85.

Carpenter, E.J., McCarthy, J.J., 1975. Nitrogen fixation and uptake of combined nitrogenous nutrients by *Oscillatoria* (*Trichodesmium*) *thiebautii* in the western Sargasso Sea. Limnology and Oceanography 20, 389–401.

Carpenter, E.J., Romans, K., 1991. Major role of the cyanobacterium *Trichodesmium* in nutrient cycling in the North Atlantic Ocean. Science 254, 1356–1358.

Carpenter, E.J., Harvey, H.R., Fry, B., Capone, D.G., 1997. Biogeochemical tracers of the marine cyanobacterium *Trichodesmium*. Deep-Sea Research, Part I 44, 27–38.

Chicarelli, M.I., Hayes, J.M., Popp, B.N., Eckardt, C.B., Maxwell, J.R., 1993. Carbon and nitrogen isotopic compositions of alkyl porphyrins from the Triassic Serpiano oil shale. Geochimica et Cosmochimica Acta 57, 1307–1311.

Cline, J.D., Kaplan, I.R., 1975. Isotopic fractionation of dissolved nitrate during denitrification in the eastern tropical North Pacific Ocean. Marine Chemistry 3, 271–299.

Coccioni, R., Luciani, V., 2004. Planktonic foraminifera and environmental changes across the Bonarelli event (OAE2, Latest Cenomanian) in its type area: a high-resolution study from the Tethyan reference Bottaccione Section (Gubbio, central Italy). Journal of Foraminiferal Research 34, 109–129.

Colman, B., 1989. Photosynthetic carbon assimilation and the suppression of photorespiration in the cyanobacteria. Aquatic Botany 34, 211–231.

Cresta, S., Monechi, S., Parisi, G., 1989. Mesozoic-Cenozoic Stratigraphy in the Umbria-Marche Area. Geological field trips in the Umbria-Marche Apennines (Italy). Memorie Descrittive della Carta Geologica d'Italia, vol. 39.

Davis, C.S., McGillicuddy Jr., D.J., 2006. Transatlantic abundance of the N_2 -fixing colonial cyanobacterium *Trichodesmium*. Science 312, 1517–1520.

Dean, W.E., Arthur, M.A., Claypool, G.E., 1986. Depletion of ^{13}C in Cretaceous marine organic-matter: Source, diagenetic, or environmental signal. Marine Geology 70, 119–157.

Descolas-Gros, C., Fontugne, M.R., 1985. Carbon fixation in marine phytoplankton: carboxylase activities and stable carbon-isotope ratios; physiological and paleoclimatological aspects. Marine Biology 87, 1–6.

Descolas-Gros, C., Fontugne, M., 1990. Stable carbon isotope fractionation by marine phytoplankton during photosynthesis. Plant, Cell and Environment 13, 207–218.

Dumitrescu, M., Brassell, S.C., 2006. Compositional and isotopic characteristics of organic matter for the early Aptian Oceanic Anoxic Event at Shatsky Rise, ODP Leg 198. Palaeogeography, Palaeoclimatology, Palaeoecology 235, 168–191.

Dupouy, C., Neveux, J., Subramaniam, A., Mulholland, M.R., Montoya, J.P., Campbell, L., Carpenter, E.J., Capone, D.G., 2000. Satellite captures *Trichodesmium* blooms in the southwestern tropical Pacific. Eos 81, 13–16.

Eckardt, C.B., Keely, B.J., Waring, J.R., Chicarelli, M.I., Maxwell, J.R., 1991. Preservation of chlorophyll-derived pigments in sedimentary organic matter. Philosophical Transactions, Royal Society of London B 333, 339–348.

Filer, C.N., 1999. Isotopic fractionation of organic compounds in chromatography. Journal of Labelled Compounds and Radiopharmaceuticals 42, 169–197.

Fogel, M.L., Cifuentes, L.A., 1993. Isotope fractionation during primary production. In: Engel, M.H., Macko, S.A. (Eds.), Organic Geochemistry. Plenum Press, New York, pp. 73–98.

Forster, A., Schouten, S., Moriya, K., Wilson, P.A., Sinninghe Damsté, J.S., 2007. Tropical warming and intermittent cooling during a mid-Cretaceous oceanic anoxic even. Paleoceanography 22, PA1219. doi:10.1029/2006PA00134.

Francois, R., Altabet, M.A., Goericke, R., McCorkle, D.C., Brunet, C., Poisson, A., 1993. Changes in the $\delta^{13}C$ of surface water particulate organic matter across the subtropical convergence in the SW Indian Ocean. Global Biogeochemical Cycles 7, 627–644.

Freeman, K.H., Hayes, J.M., 1992. Fractionation of carbon isotopes by phytoplankton and estimates of ancient CO_2 levels. Global Biogeochemical Cycles 6, 185–198.

Goericke, R., Montoya, J.P., Fry, B., 1994. Physiology of isotopic fractionation in algae and cyanobacteria. In: Lajtha, K., Michener, R.H. (Eds.), Stable Isotopes in Ecology and Environmental Science. Blackwell Science, Cambridge, pp. 187–221.

Hallam, A., Wignall, P.B., 1999. Mass extinctions and sea-level changes. Earth-Science Reviews 48, 217–250.

Hayes, J.M., 1993. Factors controlling ^{13}C contents of sedimentary organic compounds: Principles and evidence. Marine Geology 113, 111–125.

Hayes, J.M., Takigiku, R., Ocampo, R., Callot, H.J., Albrecht, P., 1987. Isotopic compositions and probable origins of organic molecules in the Eocene Messel shales. Nature 329, 48–51.

Hayes, J.M., Popp, B.N., Takigiku, R., Johnson, M.W., 1989. An isotopic study of biogeochemical relationships between carbonates and organic carbon in the Greenhorn Formation. Geochimica et Cosmochimica Acta 53, 2961–2972.

Hayes, J.M., Freeman, K.H., Popp, B.N., Hoham, C.H., 1990. Compound-specific isotopic analyses: A novel tool reconstruction of ancient biogeochemical processes. Organic Geochemistry 16, 1115–1128.

Hinga, K.R., Arthur, M.A., Pilson, M.E.Q., Whitaker, D., 1994. Carbon isotope fractionation by marine phytoplankton in culture: the effects of CO_2 concentration, pH, temperature, and species. Global Biogeochemical Cycles 8, 91–102.

Jasper, J.P., Hayes, J.M., 1990. A carbon isotope record of CO_2 levels during the late Quaternary. Nature 347, 462–464.

Jenkyns, H.C., 1980. Cretaceous anoxic events: from continents to oceans. Journal of Geological Society of London 137, 171–188.

Jenkyns, H.C., Forster, A., Schouten, S., Sinninghe Damsté, J.S., 2004. High temperatures in the Late Cretaceous Arctic Ocean. Nature 432, 888–892.

Kaplan, A., Badger, M.R., Berry, J.A., 1980. Photosynthesis and intracellular inorganic carbon pool in the blue-green algae *Anabaena variabilis*: Response to external CO_2 concentration. Planta 149, 219–226.

Kaplan, A., Reinhold, L., 1999. CO_2 -concentrating mechanisms in photosynthetic microorganisms. Annual Review of Plant Physiology and Plant Molecular Biology 50, 539–570.

Karl, D., Letelier, R., Tupas, L., Dore, J., Christian, J., Hebel, D., 1997. The role of nitrogen fixation in biogeochemical cycling in the subtropical North Pacific Ocean. Nature 386, 533–538.

Kashiyama, Y., Kitazato, H., Ohkouchi, N., 2007. An improved method for isolation and purification of sedimentary

porphyrins by high-performance liquid chromatography for compound-specific isotopic analysis. Journal of Chromatography A 1138, 73–83.

Kashiyama, Y., 2006. Reconstruction of biogeochemical environment of the past ocean based on compound-specific carbon and nitrogen isotopic compositions of sedimentary porphyrins. Ph.D. Thesis, Univ. Tokyo.

Keely, B.J., Prowse, W.G., Maxwell, J.R., 1990. The Treibs hypothesis: an evaluation based on structural studies. Energy & Fuels 4, 628–634.

Keely, B.J., Harris, P.G., Popp, B.N., Hayes, J.M., Meischner, D., Maxwell, J.R., 1994. Porphyrin and chlorin distributions in a Lake Pliocene lacustrine sediment. Geochimica et Cosmochimica Acta 58, 3691–3701.

Kohnen, M.E.L., Schouten, S., Sinninghe Damsté, J.S., De Leeuw, J.W., Merritt, D.A., Hayes, J.M., 1992. Recognition of paleobiochemicals by a combined molecular sulfur and isotope geochemical approach. Science 256, 358–362.

Kuroda, J., Ogawa, N.O., Tanimizu, M., Coffin, M.F., Tokuyama, H., Kitazato, H., Ohkouchi, N., 2007. Contemporaneous massive subaerial volcanism and Late Cretaceous oceanic anoxic event 2. Earth and Planetary Science Letters 256, 211–223.

Kuroda, J., Ohkouchi, N., Ishii, T., Tokuyama, H., Taira, A., 2005. Lamina-scale analysis of sedimentary components in Cretaceous black shales by chemical compositional mapping: Implications for paleoenvironmental changes during the Oceanic Anoxic Events. Geochimica et Cosmochimica Acta 69, 1479–1494.

Kuroda, J., Ohkouchi, N., 2006. Implications of spatiotemporal distribution of black shales during Cretaceous Oceanic Anoxic Event-2. Paleontological Research 10, 345–358.

Kuypers, M.M.M., Pancost, R.D., Sinninghe Damsté, J.S., 1999. A large and abrupt fall in atmospheric CO_2 concentration during Cretaceous times. Nature 399, 342–345.

Kuypers, M.M.M., Blokker, P., Erbacher, J., Kinkel, H., Pancost, R.D., Schouten, S., Sinninghe Damsté, J.S., 2001. Massive expansion of marine archaea during a mid-Cretaceous oceanic anoxic event. Science 293, 92–94.

Kuypers, M.M.M., Pancost, R.D., Nijenhuis, I.A., Sinninghe Damsté, J.S., 2002. Enhanced productivity led to increased organic carbon burial in the euxinic North Atlantic basin during the late Cenomanian oceanic anoxic event. Paleoceanography 17, 1051. doi:10.1029/2000PA000569.

Kuypers, M.M.M., van Breugel, Y., Schouten, S., Erba, E., Sinninghe Damsté, J.S., 2004. N_2 -fixing cyanobacteria supplied nutrient N for Cretaceous oceanic anoxic events. Geology 32, 853–856.

Liu, K.-K., Kaplan, I.R., 1989. The eastern tropical Pacific as a source of ^{15}N-enriched nitrate in seawater off southern California. Limnology and Oceanography 34, 820–830.

Marumo, R., Asaoka, O., 1974. Distribution of pelagic blue-green algae in the North Pacific Ocean. Journal of Oceanographic Society of Japan 30, 77.

Mau, Y.-H.L., Wang, W.-Y., 1988. Biosynthesis of δ-aminolevulnic acid in *Chlamidomonas reinhardtii*: study of transamilation mechanism using specifically labeled glutamate. Plant Physiology 86, 793–797.

Mayer, S.M., Gawlita, E., Avissar, Y.J., Anderson, V.E., Beale, S.I., 1993. Intermolecular nitrogen transfer in the enzymic conversion of glutamate to δ-aminolevulnic acid by extracts of *Chlorella vulgaris*. Plant Physiology 101, 1029–1038.

Meyers, S.R., Sageman, B.B., Hinnov, L.A., 2001. Integrated quantitative stratigraphy of Cenomanian-Turonian Bridge Creek Limestone Member using evolutive harmonic analysis and stratigraphic modeling. Journal of Sedimentary Research 71, 628–644.

Miyake, Y., Wada, E., 1967. The abundance ratio of $^{15}N/^{14}N$ in marine environments. Records of Oceanographic Works in Japan 9, 37–53.

Montoya, J.P., Holl, C.M., Zehr, J.P., Hansen, A., Villareal, T.A., Capone, D.G., 2004. High rates of N_2 fixation by unicellular diazotrophs in the oligotrophic Pacific Ocean. Nature 430, 1027–1031.

Mook, W.G., Bommerson, J.C., Staberman, W.H., 1974. Carbon isotope fractionation between dissolved bicarbonate and gaseous carbon dioxide. Earth and Planetary Science Letters 22, 169–176.

Needoba, J.A., Waser, N.A., Harrison, P.J., Calvert, S.E., 2003. Nitrogen isotope fractionation in 12 species of marine phytoplankton during growth on nitrate. Marine Ecology-Progress Series 255, 81–91.

Ocampo, R., Callot, H.J., Albrecht, P., Popp, B.N., Horowitz, M.R., Hayes, J.M., 1989. Different isotope compositions of C_{32} DPEP and C_{32} etioporphyrin III in oil shale. Naturwissenschaften 76, 419–421.

Ogawa, T., Kaplan, A., 2003. Inorganic carbon acquisition systems in cyanobacteria. Photosynthesis Research 77, 105–115.

Ogawa, T., 1993. Molecular analysis of the CO_2 concentrating mechanism in cyanobacteria. In: Yamamoto, H.Y., Smith, C. (Eds.), Photosynthetic Responses to the Environment. American Society of Plant Physiologist, Rockville, pp. 113–125.

Ohkouchi, N., Kawamura, K., Wada, E., Taira, A., 1997. High abundances of hopanols and hopanoic acids in Cretaceous black shales. Ancient Biomolecules 1, 183–192.

Ohkouchi, N., Nakajima, Y., Okada, H., Ogawa, N.O., Suga, H., Oguri, K., Kitazato, H., 2005. Biogeochemical processes in a meromictic lake Kaiike: Implications from carbon and nitrogen isotopic compositions of photosynthetic pigments. Environmental Microbiology 7, 1009–1016.

Ohkouchi, N., Kashiyama, Y., Kuroda, J., Ogawa, N.O., Kitazato, H., 2006. An importance of cyanobacteria as a primary producer during Cretaceous Oceanic Anoxic Event 2. Biogeosciences 3, 467–478.

Ohkouchi, N., Nakajima, Y., Ogawa, N.O., Chikaraishi, Y., Suga, H., Sakai, S., Kitazato, H., 2007. Carbon isotopic composition of the tetrapyrrole nucleus in chloropigments from a saline meromictic lake: A mechanistic view for interpreting the isotopic signature of alkyl porphyrins in geological samples. Organic Geochemistry. doi:10.1016/j.orggeochem.2007.11.002.

O'Leary, M.H., Madhaven, S., Paneth, P., 1992. Physical and chemical basis of carbon isotope fractionation in plants. Plant, Cell and Environment 15, 1099–1104.

Pagani, M., Arthur, M.A., Freeman, K.H., 1999a. Miocene evolution of atmospheric carbon dioxide. Paleoceanography 14, 273–292.

Pagani, M., Freeman, K.H., Arthur, M.A., 1999b. Late Miocene atmospheric CO_2 concentrations and the expansion of C_4 grasses. Science 285, 876–879.

Pagani, M., Freeman, K.H., Ohkouchi, N., Caldeira, K., 2002. Comparison of water column $[CO_{2aq}]$ with sedimentary

alkenone-based estimates: A test of the alkenone-CO_2 proxy. Paleoceanography 17, 1069. doi:10.1029/2002PA000756.

Pancost, R.D., Freeman, K.H., Wakeham, S.G., Robertson, C.Y., 1997. Controls on carbon isotope fractionation by diatoms in the Peru upwelling region. Geochimica et Cosmochimica Acta 61, 4983–4991.

Pancost, R.D., Crawford, N., Magness, S., Turner, A., Jenkyns, H.C., Maxwell, J.R., 2004. Further evidence for the development of photic-zone euxinic conditions during Mesozoic oceanic anoxic events. Journal of the Geological Society, London 161, 353–364.

Pederson, T.F., Calvert, S.E., 1991. Anoxia vs productivity: What controls the formation of organic-carbon-rich sediments and sedimentary rocks? American Association of Petroleum Geologists Bulletin 74, 454–466.

Philip, J., Babinot, J.F., Tronchetti, G., Fourcade, E., Azema, J., Guiraud, R., Bellion, Y., Ricou, L.E., Vrielynck, B., Boulin, J., Cornee, J.J., Herbin, J.P., 1993. Late Cenomanian palaeoenvironments (94.92 Ma). In: Dercourt, J., Ricou, L.E., Vrielynck, B. (Eds.), Atlas Tethys Palaeoenvironmental Maps, Explanatory Notes. Gauthier-Villars, Paris, pp. 153–178.

Philip, J., Babinot, J.F., Tronchetti, G., Fourcade, E., Ricou, L.E., Guiraud, R., Bellion, Y., Herbin, J.P., Combes, P.J., Cornee, J.J., Decourt, J., 2000. Late Cenomanian. In: Dercourt, J., Ricou, L.E., Vrielynck, B. (Eds.), Atlas Peri-Tethys, Palaeogeographical Maps. CCGM/CGMW, Paris, Map 14.

Pratt, L.M., 1984. Influence of paleoenvironmental factors on preservation of organic matter in the mid-Cretaceous Greenhorn Formation, Pueblo, Colorado. American Association of Petroleum Geologists Bulletin 68, 1146–1159.

Popp, B.N., Takigiku, R., Hayes, J.M., Louda, J.W., Baker, E.W., 1989. The post-Paleozoic chronology and mechanism of ^{13}C depletion in primary marine organic matter. American Journal of Science 289, 436–454.

Popp, B.N., Laws, E.A., Bidigare, R.R., Dore, J.E., Hanson, K.L., Wakeham, S.G., 1998. Effect of phytoplankton cell geometry on carbon isotopic fractionation. Geochimica et Cosmochimica Acta 62, 69–77.

Popp, B.N., Trull, T., Kenig, F., Wakeham, S.G., Rust, T.M., Tilbrook, B., Griffiths, F.B., Wright, S.W., Marchant, H.J., Bidigare, R.R., Laws, E.A., 1999. Controls on the carbon isotopic composition of Southern Ocean phytoplankton. Global Biogeochemical Cycles 13, 827–844.

Rau, G.H., Takahashi, T., Des Marais, D.J., Repeta, D.J., Martin, J.H., 1992. The relationship between $\delta^{13}C$ of organic matter and $[CO_2(aq)]$ in ocean surface water: Data from a JGOFS site in the northeast Atlantic Ocean and a model. Geochimica et Cosmochimica Acta 56, 1413–1419.

Raven, J.A., 1997. Inorganic carbon acquisition by marine autotrophs. In: Callow, J.A. (Ed.), Advances in Botanical Research, vol. 27. Academic Press, pp. 85–209.

Sachs, J.P., Repeta, D.J., 1999a. Oligotrophy and nitrogen fixation during eastern Mediterranean sapropel events. Science 286, 2485–2488.

Sachs, J.P., Repeta, D.J., Goericke, R., 1999b. Nitrogen and carbon isotopic ratios of chlorophyll from marine phytoplankton. Geochimica et Cosmochimica Acta 63, 1431–1441.

Saino, T., Hattori, A., 1987. Geographical variation of the water column distribution of suspended particulate organic nitrogen and its ^{15}N natural abundance in the Pacific and its marginal seas. Deep Sea Research, Part A 34, 807–827.

Sakata, S., Hayes, J.M., McTaggart, A.R., Evans, R.A., Leckrone, K.J., Togasaki, R.K., 1997. Carbon isotopic fractionation associated with lipid biosynthesis by a cyanobacterium: Relevance for interpretation of biomarker records. Geochimica et Cosmochimica Acta 61, 5379–5389.

Schlanger, S.O., Jenkyns, H.C., 1976. Cretaceous oceanic anoxic events – causes and consequences. Geologie en Mijnbouw 55, 179–184.

Schlanger, S.O., Arthur, M.A., Jenkyns, H.C., Scholle, P.A., 1987. The Cenomanian–Turonian Oceanic Anoxic Event, I. Stratigraphy and distribution of organic carbon-rich beds and the marine $\delta^{13}C$ excursion. In: Brooks, J., Fleet, A.J. (Eds.), Marine and Petroleum Source Rocks, vol. 26. Geological Society Special Publications, pp. 371–399.

Schouten, S., Hopmans, E.C., Forster, A., van Breugel, Y., Kuypers, M.M.M., Sinninghe Damsté, J.S., 2003. Extremely high sea-surface temperatures at low latitudes during the middle Cretaceous as revealed by archaeal membrane lipids. Geology 31, 1069–1072.

Scotese, C.R., Golonka, J., 1992. Paleogeographic Atlas. University of Texas, Arlington.

Sharkey, T., Berry, J.A., 1985. Carbon isotope fractionation of algae as influenced by an inducible CO_2 concentrating mechanism. In: Lucas, W.J., Berry, J.A. (Eds.), Inorganic Carbon Uptake by Aquatic Photosynthetic Organisms. American Society of Plant Physiology, Rockville, MD, pp. 389–402.

Sigman, D.M., Altabet, M.A., McCorkle, D.C., Francois, R., Fischer, G., 2000. The $\delta^{15}N$ of nitrate in the Southern Ocean: Nitrogen cycling and circulation in the ocean interior. Journal of Geophysical Research 105, 19, 59.

Sigman, D.M., Robinson, R., Knapp, A.N., van Geen, A., McCorkle, D.C., Brandes, J.A., Thunell, R.C., 2003. Distinguishing between water column and sedimentary denitrification in the Santa Barbara Basin using the stable isotopes of nitrate. Geochemistry, Geophysics, Geosystems 4, 1040.

Smith, B.N., Epstein, S., 1971. Two categories of $^{13}C/^{12}C$ ratios for higher plants. Plant Physiology 47, 380–384.

Summons, R.E., Jahnke, L.L., Hope, J.M., Logan, G.A., 1999. 2-Methylhopanoids as biomarkers for cyanobacterial oxygenic photosynthesis. Nature 400, 554–557.

Sutka, R.L., Ostrom, N.E., Ostrom, P.H., Phanikumar, M.S., 2004. Stable nitrogen isotope dynamics of dissolved nitrate in a transect from the North Pacific Subtropical Gyre to the Eastern Tropical North Pacific. Geochimica et Cosmochimica Acta 68, 517–527.

Tabita, F.R., 1993. Biochemistry and molecular regulation of carbon dioxide metabolism in cyanobacteria. In: Bryant, D.A. (Ed.), The Molecular Biology of Cyanobacteria. Kluwer Academic Publishers, Netherland, pp. 437–467.

Tajika, E., 1998. Climate change during the last 150 million years: reconstruction from a carbon cycle model. Earth and Planetary Science Letters 160, 695–707.

Thode, H.G., Shima, M., Rees, C.E., Krishnamurthy, K.V., 1965. Carbon-13 isotope effects in systems containing carbon dioxide, bicarbonate, carbonate, and metal ions. Canadian Journal of Chemistry 43, 582–589.

Treibs, A., 1936. Chlorophyll and hemin derivatives in organic materials. Angewandte Chemie 49, 682–686.

Voss, M., Dippner, J.W., Montoya, J.P., 2001. Nitrogen isotope patterns in the oxygen-deficient waters of the eastern tropical North Pacific Ocean. Deep Sea Research, Part I 48, 1905–1921.

Wada, E., Hattori, A., 1978. Nitrogen isotope effects in the assimilation of inorganic nitrogenous compounds by marine diatoms. Geomicrobiology Journal 1, 85–101.

Wada, E., Hattori, A., 1991. Nitrogen in the Sea: Forms, Abundances, and Rate Processes. CRC Press, Boca Raton.

Waser, N.A.D., Harrison, P.J., Nielsen, B., Calvert, S.E., 1998. Nitrogen isotope fractionation during the uptake and assimilation of nitrate, nitrite, ammonium, and urea by a marine diatom. Limnology and Oceanography 43, 215–224.

York, J.K., Tomasky, G., Valiela, I., Repeta, D.J., 2007. Stable isotopic detection of ammonium and nitrate assimilation by phytoplankton in the Waquoit Bay estuarine system. Limnology and Oceanography 52, 144–155.

Zehr, J., Waterbury, J., Turner, P., Montoya, J., Omoregie, E., Steward, G., Hansen, A., Karl, D., 2001. Unicellular cyanobacteria fix N_2 in the subtropical North Pacific Ocean. Nature 412, 635–638.